General Relativistic Simulations of Binary Neutron Star Mergers

Bruno Giacomazzo[*,†], Luciano Rezzolla[**], Luca Baiotti[‡], David Link[**,§] and José A. Font[¶]

[*]*Department of Astronomy, University of Maryland, College Park, MD, USA*
[†]*Gravitational Astrophysics Laboratory, NASA Goddard Space Flight Center, Greenbelt, MD, USA*
[**]*Max-Planck-Institut für Gravitationsphysik, Albert-Einstein-Institut, Potsdam-Golm, Germany*
[‡]*Institute of Laser Engineering, Osaka University, Suita, Japan*
[§]*Institut für Physik, Humboldt-Universität zu Berlin, Berlin, Germany*
[¶]*Departamento de Astronomía y Astrofísica, Universitat de València, Valencia, Spain*

Abstract. Binary neutron star mergers are one of the possible candidates for the central engine of short gamma-ray bursts (GRBs) and they are also powerful sources of gravitational waves. We have used our fully general relativistic hydrodynamical code `Whisky` to investigate the merger of binary neutron star systems and we have in particular studied the properties of the tori that can be formed by these systems, their possible connection with the engine of short GRBs and the gravitational wave signals that detectors such as advanced LIGO will be able to detect. We have also shown how the mass of the torus varies as a function of the total mass of the neutron stars composing the binary and of their mass ratio and we have found that tori sufficiently massive to power short GRBs can indeed be formed.

Keywords: neutron stars, gravitational waves, gamma-ray bursts, numerical relativity
PACS: 04.30.Db, 04.40.Dg, 04.70.Bw, 95.30.Lz, 97.60.Jd

INTRODUCTION

The numerical investigation in full general relativity (GR) of the merger of binary neutron stars (BNSs) has produced a series of new and interesting results in the last years (see [1] for a recent review). Thanks to several numerical improvements, it has been indeed possible to start to investigate the full dynamics of these systems including the formation of tori around rapidly rotating black holes (BHs) (e.g., see [2, 3]) which could not be modeled via Newtonian simulations. This progress has allowed the beginning of an accurate investigation of whether BNS mergers could indeed be behind the central engine of short γ-ray bursts (GRBs) [4, 5]. The consensus emerging from the existing simulations suggests the formation of a spinning BH surrounded by a hot disk. Driven by neutrino processes and magnetic fields, such a compact system may be capable of launching a relativistic fireball with an energy of $\sim 10^{48}$ erg on a timescale of $0.1-1$ s [6]. Moreover, BNSs are also one of the most powerful sources of gravitational waves (GWs) that will be detected in the next few years by advanced LIGO and advanced Virgo [7]. GR simulations of BNSs have then started to provide accurate templates that can be used to infer properties of the NSs composing the binaries, such as the equation of state (EOS) of NSs, once their GWs will be detected [8]. Here we review some of the main results published in [9] where we studied the evolution of BNSs with different masses and different mass ratios. We will show not only the dynamics and the GWs generated by these systems, but also that unequal-mass binaries can indeed produce tori sufficiently massive to possibly power short GRBs.

NUMERICAL AND PHYSICAL SETUP

All the details of the mathematical and numerical setup used for producing the results presented here are discussed in [9] and here we limit ourselves to a brief overview. We have used the `Whisky` code [10, 11] which solves the equations of general relativistic hydrodynamics on dynamical curved backgrounds. In particular `Whisky` makes use of the `Cactus` framework which provides the evolution of the Einstein equations for the metric expressed in the BSSN formulation [12]. The hydrodynamic equations are instead solved using high resolution shock capturing schemes and in particular by using the Marquina flux formula and the Piecewise Parabolic Method [2, 9]. The system

Gamma Ray Bursts 2010
AIP Conf. Proc. 1358, 187-190 (2011); doi: 10.1063/1.3621768

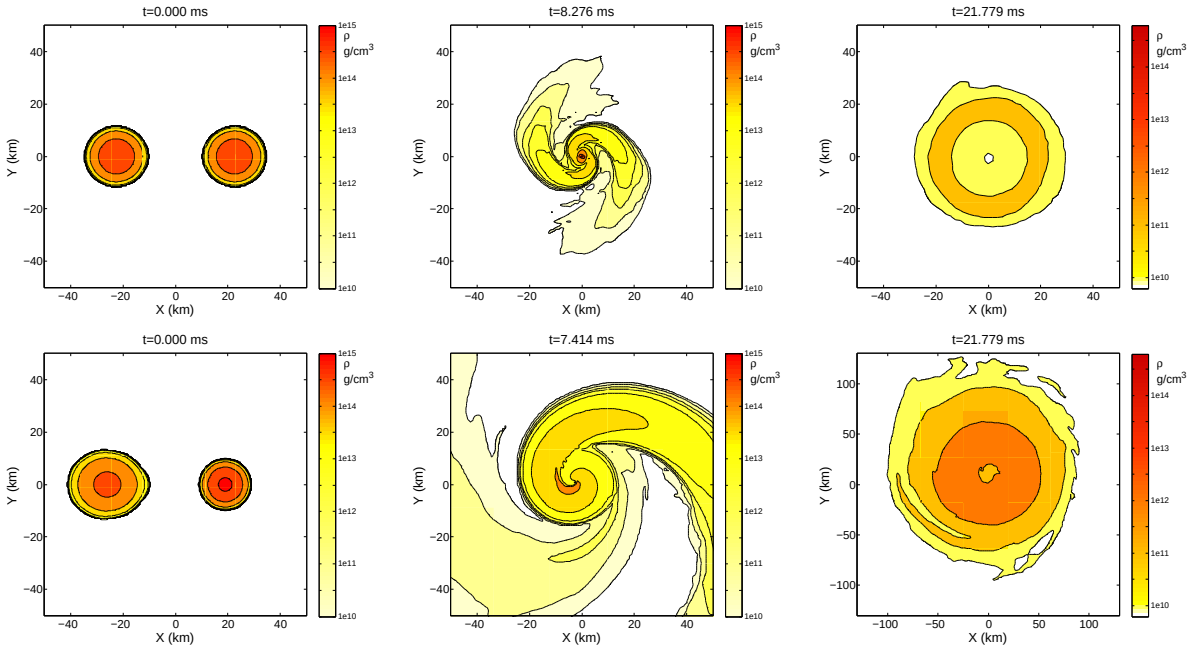

FIGURE 1. Isodensity contours for the equal-mass model `M3.6q1.00` (top panels) and the unequal-mass binary `M3.4q0.70` (bottom panels) on the (x,y) plane. The times when the frames have been taken are shown on top of the plots while the colour code for the rest-mass density is indicated to the right of each plot. Figure taken from [9].

of hydrodynamics equations is closed by an EOS and here we adopt the commonly used "ideal-fluid" EOS, in which the pressure p is expressed as $p = \rho\,\varepsilon(\Gamma - 1)$, where ρ is the rest-mass density, ε is the specific internal energy, and $\Gamma = 2$ is the adiabatic exponent.

The `Whisky` code implements adaptive mesh refinement by using the `Carpet` driver [13]. The grid resolution varies from $\Delta_6 \sim 221\,\mathrm{m}$ for the finest level, which covers completely each star during the inspiral, to $\Delta_1 \sim 7.1\,\mathrm{km}$ for the coarsest level, whose outer boundary is at $\sim 360\,\mathrm{km}$ [9].

Finally, the initial data are generated with the multi-domain spectral-method code `LORENE` [14] and details about the physical properties of the different binaries can be found in [9].

RESULTS

Figure 1 shows some snapshots of the evolution of two of the six binaries evolved in [9]: `M3.6q1.00` (top panels) and `M3.4q0.70` (bottom panels). It shows in particular the rest-mass density on the equatorial plane at different times. The first column shows the initial conditions, the second one the collapse to BH of the hypermassive NS formed after the merger and the last one the torus formed at the end of the simulations. Note in particular the very different length scale between the two panels in the last column. From Fig. 1 it is clearly evident the different dynamics between the equal-mass case (`M3.6q1.00`) and the unequal-mass one (`M3.4q0.70`). In the latter, the less massive star is tidally disrupted during the inspiral and produce a tidal tail (see bottom panel in the second column). Most of the matter in the tail is bounded and will fall back on the torus at a later time. Because of the tidal disruption more matter is deposited in the torus which is more massive, with higher densities and with a larger extension compared to the one formed after the merger of the equal mass case (compare the two panels in the last column and note the very different length scale).

The fraction of the total mass of the system that remains outside the BH is shown in the left panel of Fig. 2 for all the six binaries considered in [9]. From this figure it is in particular evident that binaries with lower mass ratios form in general more massive tori. In the right panel of Fig. 2 we also show the total mass of the torus as a function of both the total mass of the system $M_{\rm tot}$ and of the mass ratio q. The dependence of the mass of the torus from the mass ratio and the total mass of the binary can be represented with this phenomenological expression [9]:

$$\widetilde{M}_{\rm tor}(q, M_{\rm tot}) = [c_3(1+q)M_* - M_{\rm tot}]\,[c_1(1-q) + c_2]\,, \qquad (1)$$

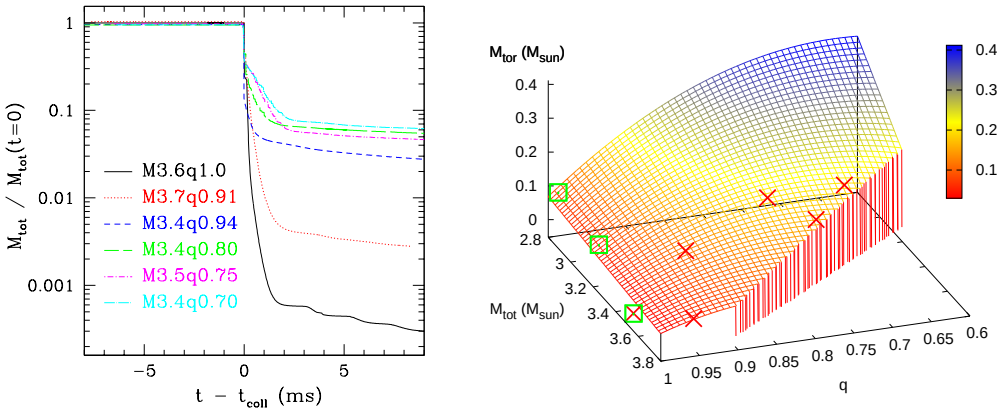

FIGURE 2. *Left panel:* evolution of the total rest masses $M_{\rm tot}$ normalized to their initial values for all the models considered in [9]. The curves referring to different models have been shifted in time to coincide at the time of the formation of the BH ($t_{\rm coll}$). *Right panel:* different symbols show the torus mass $M_{\rm tor}$ measured either in the simulations reported in [9] (red crosses) or in those reported in [2] (green squares). Also shown in the parameter space $(q, M_{\rm tot})$ considered here is the phenomenological modeling $\widetilde{M}_{\rm tor}$ suggested by expression (1). Note that to highlight the functional behavior of the phenomenological expression, the $x-$ and $y-$axes are shown as decreasing when moving to the right and to the left, respectively. Figure taken from [9].

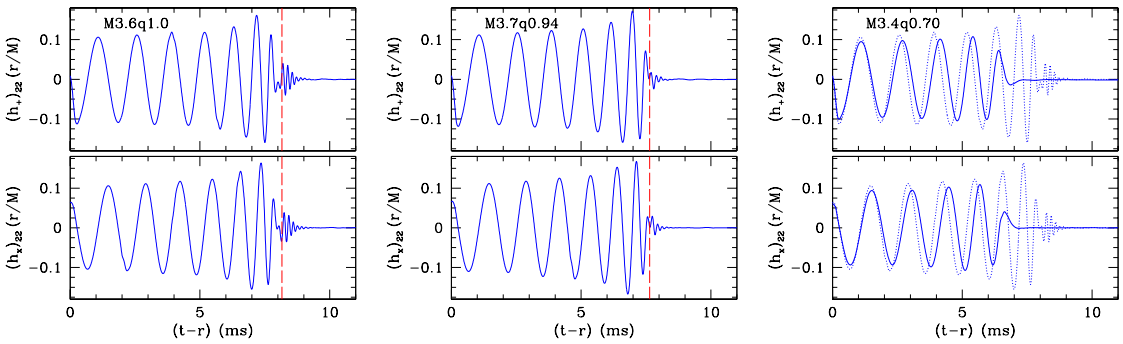

FIGURE 3. Gravitational waveforms in the two polarizations h_+ (upper panels) and $h_\times$ (lower panels) as computed from the lowest $\ell = m = 2$ multipole for three of the six binaries considered in [9]. For those models where it was found, the vertical dashed lines mark the time of the first detection of the apparent horizon. Note that as the mass ratio q decreases, the ringdown part of the signal starts earlier but it is also less evident because of the increasingly large accretion after the formation of the apparent horizon. Finally, shown as an aid to comparison, the panel of the binary `M3.4q070` also reports with dotted lines the waveforms for the equal-mass binary `M3.6q1.00`. Figure taken from [9].

where M_* is the maximum mass of an isolated nonrotating star. The three coefficients, c_1, c_2, and c_3 can be computed by comparing expression (1) with the numerical data reported in [2, 9]. The fitting procedure then yields $c_1 = 1.115 \pm 1.090, c_2 = 0.039 \pm 0.023, c_3 = 1.139 \pm 0.149$, with a reduced $\chi^2 \simeq 2 \times 10^{-3}$. The right panel of Fig. 2 shows the torus mass against the phenomenological modeling $\widetilde{M}_{\rm tor}$ suggested by expression (1) in the region where the total mass of the binary is smaller then the allowed maximum mass, as well as the numerical results (red crosses and green squares). It is evident from this figure that equal-mass ($q = 1$) systems with a very high total mass form very small tori (e.g., model `M3.6q1.00` produces a torus with mass $M_{\rm tor} \approx 0.001 M_\odot$). On the other hand, BNSs with a lower total mass and lower mass ratios can form tori sufficiently massive to power short GRBs. In particular, tori with masses $\lesssim 0.21 M_\odot$ have been measured in our simulations and even more massive ones, i.e. with masses up to $\sim 0.35 M_\odot$, are possible for mass ratios $q \sim 0.75 - 0.85$.

Finally Fig. 3 shows the GW signal emitted by three of the six models studied in [9]. The signal is composed by the inspiral, merger and ringdown of the black hole (i.e., the part of the signal at the right of the vertical dashed line

in the first two panels). In particular note that as the mass ratio q decreases (i.e. going from the equal-mass case in the left panel to the unequal-mass cases in the right panels), the ringdown part of the signal starts earlier, but it is also less evident because of the more massive tori and of the increasingly large accretion after the formation of the BH. This is an example of how GW signals contain information about the formation or not of massive tori that could be sufficient to power short GRBs. It is also important to stress that such signals would be detectable by advanced LIGO and advanced Virgo up to distances of ~ 100 Mpc [9].

CONCLUSIONS

We have presented some of the main results published in [9] regarding the merger of binary NSs in general relativity. We have shown that when considering binaries with unequal masses it is possible to form very large and massive tori with masses larger than $0.01M_{\odot}$ and even as large as $\sim 0.2M_{\odot}$ which would then be sufficient to power short GRBs. We have also derived an empirical relation between the mass of the torus and the total mass and mass ratio of the binary. In order to produce sufficiently massive tori it is necessary to go toward lower total masses and low mass ratios. We have also computed the GW signal emitted by these systems and shown as some of its features, e.g. the suppression of the ringdown part of the signal, are directly related to the formation of a massive torus. Further numerical simulations of these systems in full general relativity, including also the presence of magnetic fields [15, 16] and the emission of neutrinos, will help to determine the link between BNSs and the engine of short GRBs [17].

ACKNOWLEDGMENTS

It is a pleasure to thank the group in Meudon (Paris) for producing and making available the initial data used in these calculations and also in particular to Dorota Gondek-Rosińska for essential help in building some of the initial models. We are also grateful to E. Schnetter and all the `Carpet/Cactus` developers. We finally thank Gian Mario Manca for help in producing some of the figures. The computations were performed on the Damiana cluster at the AEI, on the MareNostrum cluster at the Barcelona Supercomputing Center and on the Ranger cluster at the Texas Advanced Computing Center through TERAGRID allocation TG-MCA02N014. This work was supported in part by the DFG grant SFB/Transregio 7, by "CompStar", a Research Networking Programme of the European Science Foundation, by the JSPS Postdoctoral Fellowship For Foreign Researchers, Grant-in-Aid for Scientific Research (19-07803), by the Spanish Ministerio de Educación y Ciencia (AYA 2007-67626-C03-01), and by NASA grant number NNX09AI75G.

REFERENCES

1. M. D. Duez, *Class. Quantum Grav.* **27**, 114002 (2010).
2. L. Baiotti, B. Giacomazzo, and L. Rezzolla, *Phys. Rev. D* **78**, 084033 (2008).
3. K. Kiuchi, Y. Sekiguchi, M. Shibata, and K. Taniguchi, *Phys. Rev. Lett.* **104**, 141101 (2010).
4. R. Narayan, B. Paczynski, and T. Piran, *Astrophys. J.* **395**, L83 (1992).
5. B. Zhang, and P. Meszaros, *Int. J. Mod. Phys. A* **19**, 2385 (2004).
6. T. Piran, *Rev. Mod. Phys.* **76**, 1143–1210 (2004).
7. K. Belczynski, R. E. Taam, V. Kalogera, F. Rasio, and T. Bulik, *Astrophys. J.* **662**, 504 (2007).
8. J. S. Read, C. Markakis, M. Shibata, K. Uryu, J. D. E. Creighton, and J. L. Friedman, *Phys. Rev. D* **79**, 124033 (2009).
9. L. Rezzolla, L. Baiotti, B. Giacomazzo, D. Link, and J.-A. Font, *Class. Quantum Grav.* **27**, 114105 (2010).
10. L. Baiotti, I. Hawke, P. Montero, and L. Rezzolla, "A new three-dimensional general-relativistic hydrodynamics code," in *Computational Astrophysics in Italy: Methods and Tools*, edited by R. Capuzzo-Dolcetta, MSAIt, Trieste, 2003, vol. 1, p. 210.
11. L. Baiotti, I. Hawke, P. J. Montero, F. Löffler, L. Rezzolla, N. Stergioulas, J. A. Font, and E. Seidel, *Phys. Rev. D* **71**, 024035 (2005).
12. D. Pollney, C. Reisswig, L. Rezzolla, B. Szilágyi, M. Ansorg, B. Deris, P. Diener, E. N. Dorband, M. Koppitz, A. Nagar, and E. Schnetter, *Phys. Rev. D* **76**, 124002 (2007).
13. E. Schnetter, S. H. Hawley, and I. Hawke, *Class. Quantum Grav.* **21**, 1465–1488 (2004).
14. E. Gourgoulhon, P. Grandclément, K. Taniguchi, J. A. Marck, and S. Bonazzola, *Phys. Rev. D* **63**, 064029 (2001).
15. B. Giacomazzo, L. Rezzolla, and L. Baiotti, *Mon. Not. R. Astron. Soc.* **399**, L164–L168 (2009).
16. B. Giacomazzo, L. Rezzolla, and L. Baiotti, *arXiv:1009.2468* (2010).
17. L. Rezzolla, B. Giacomazzo, L. Baiotti, J. Granot, C. Kouveliotou, and M. A. Aloy, *arXiv:1101.4298* (2011).